Med Bio Eng Comput (2006) 44:945-958
DOI 10.1007/s11517-006-0116-3

ORIGINAL ARTICLE

Extraction of cognitive activity-related waveforms from functional near-infrared spectroscopy signals

Ceyhun Burak Akgül · Ata Akin · Bülent Sankur

Received: 31 March 2006 / Accepted: 28 September 2006 / Published online: 24 October 2006

Abstract We address the problem of prototypical waveform extraction in cognitive experiments using functional near-infrared spectroscopy (fNIRS) signals. These waveform responses are evoked with visual stimuli provided in an oddball type experimental protocol. As the statistical signal-processing tool, we consider the linear signal space representation paradigm and use independent component analysis (ICA). The assumptions underlying ICA is discussed in the light of the signal measurement and generation mechanisms in the brain. The ICA-based waveform extraction is validated based both on its conformance to the parametric brain hemodynamic response (BHR) model and to the coherent averaging technique. We assess the intra-subject and inter-subject waveform and parameter variability.

Keywords Functional near-infrared spectroscopy · Brain hemodynamic response · Independent component analysis

1 Introduction

The main objective of most neuroimaging studies has been the precise and accurate detection of the evoked responses to single-event trial stimulation. Since the evoked responses are usually minute in amplitude, and deeply buried under the background activity of the brain, researchers have to resort to advanced signal-processing techniques to extract these evoked responses. A promising new neuroimaging modality is the functional near-infrared spectroscopy (fNIRS), which can capture cerebrovascular changes in the surface of the cortex. fNIRS can potentially detect and track cerebrovascular changes, called blood oxygenation dependent (BOLD) signals by the use of optical methods. Similar to fMRI, fNIRS is sensitive to deoxyhemoglobin (Hb) while complimentarily it can measure the changes in oxyhemoglobin (HbO_2).

Use of fNIRS is proving to be effective as a bedside instrument as well as a research tool both in neuroimaging and cancer studies. The significance of the findings of fNIRS signals vis-à-vis their fMRI counterpart is still under discussion. However, a recent study has demonstrated that strong correlations exist between BOLD–fMRI data and diffuse optical HbO_2 data [32]. In other words, functional neuroimaging studies performed by both fMRI and fNIRS methods have confirmed that the increase of regional cerebral blood flow towards activated areas exceeds the regional oxygen consumption, and hence the signal pattern observed in the BOLD response resembles the HbO_2 signal of fNIRS [27, 32, 35]. Similar to fMRI signal analysis, fNIRS analysis is concerned with the varying cerebrovascular alterations due to stimuli. These are termed as brain hemodynamic response (BHR) and they tend to last several seconds. The cerebrovascular alterations observed in all these modalities are believed to be an amalgam of various physiological components involved in the neuro-vascular coupling mechanism of the brain. Several authors

C. B. Akgül · B. Sankur
Department of Electrical and Electronics Engineering, Boğaziçi University, Istanbul, Turkey

A. Akin (✉)
Institute of Biomedical Engineering, Boğaziçi University, Bebek, Istanbul 34342, Turkey
e-mail: ata.akin@boun.edu.tr

have proposed that the underlying components of BOLD and fNIRS signals can be the changes due to heart rate variability, blood pressure, breathing, arterial pulse and even thermoregulation of the brain along with the BHR that can be evoked by a stimulus.

The groundwork for brain fNIRS studies, has already been done by several research groups over the last two decades. Delpy et al. [11, 12] have addressed the issues of tissue characterization, optical path length determination and monitoring of cerebral blood flow mechanisms. Villringer et al. [27–29, 31, 35] reported their studies on the brain's response to visual and motor stimuli. Toronov et al. [33, 34] and Obrig et al. [28] have focused on the spectral changes of hemodynamic response observed during functional activation tasks.

fMRI literature have been investigating the use of various signal processing and modeling approaches in decomposing the BOLD signal to its components in the hope of better estimating the BHR signal. The interference of heart rate variability signal along with other vascular oscillations due to breathing, arterial pulsation and even the Mayer's wave has been the major challenge in the choice of the optimum signal decomposition algorithms [5, 6, 8, 9, 13, 23, 37]. The holy grail of neuroimaging studies has been the extraction of the BHR signal hidden inside many other physiological context signals, parameterize and quantify the BHR response to a stimulus, and correlate the estimated parameters with certain behavioral features (reaction times, number of correct and wrong answers, etc). Functional near-infrared spectroscopy modality has yet to reach this maturity level in data analysis, though some distance has been covered by spectral analysis methods in resolving of fNIRS signal components [17, 26, 28–31, 33, 34]. The data acquisition methods of fNIRS and fMRI are different, yet complimentary. There is definitely a challenge and an interest in developing signal analysis techniques suitable for fNIRS signals in a competitor role to fMRI techniques and beyond.

In this work, we intend to develop a framework to process event-related fNIRS signals evoked during a target categorization task. To this end, we use independent component analysis (ICA) as a statistical signal-processing tool [16]. The data consist of short-time HbO_2 signals obtained from optical absorption measurements. ICA bases will constitute a linear signal subspace where the evoked fNIRS signals are projected. We conjecture that each basis vector in the ICA representation corresponds to one of the following physiological phenomena: (1) a cognitive activity-related waveform, that is, the fNIRS counterpart of the brain hemodynamic response (BHR); (2) a signal corresponding to baseline physiological changes in the brain and (3) all other nuisance factors due to breathing, vasomotion, noise and movement artifacts and other unaccounted activities. We use a model-guided identification method for extracting the BHR. In other words, the extracted basis vectors are sorted with respect to their conformance to the so-called Gamma model waveform. Such a model-based approach has been proposed in fMRI studies, where time-averaged BOLD [8, 13, 20, 21, 37] responses have typically yielded a bell-shaped curve skewed towards its falling side as in Fig. 1.

Within the experimental protocol, the stimulus intervals are predefined and, in addition, the time span of the evoked responses is assumed known [1, 6, 9, 10]. The recorded data consist of optical absorption measurements, captured from several detectors on the prefrontal cortex, as described in more detail in Sect. 2. We should note that there is no guarantee for the cognitive response, if any, to appear on all detectors. In fact, the very purpose of our exploratory analysis is to extract signal patterns corresponding to evoked BHR in certain spatial or temporal locations. These patterns may appear in a subset of detectors in a given time epoch, depending for example on the vascularization of the region, or over several epochs in one or more spatial locations. With this goal in mind, we form fNIRS–HbO_2 datasets for each monitored brain region with measurements obtained from subjects and extract cognitive activity-related waveforms. Materials and methods as well as previous work are presented in Sect. 2. In Sect. 3, we present the results of our findings in different aspects. In Sects. 4 and 5, we discuss the

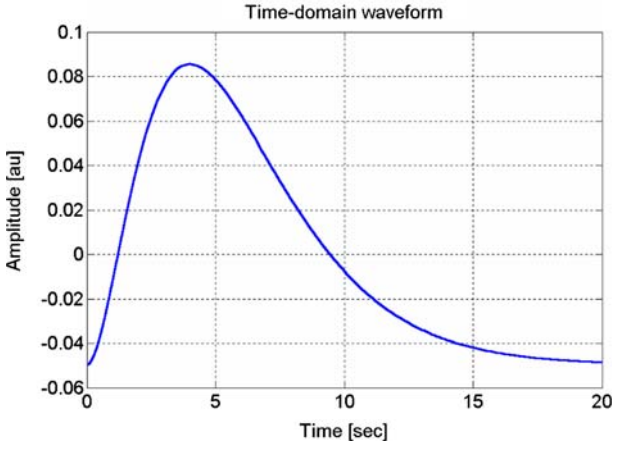

Fig. 1 Gamma model waveform, $h(t) = B(t-T)^2 e^{-(t-T)/\tau}$, $t > T$, where $B = 1/\tau^3$, $T = 0$, $\tau = 2$. The mean of the signal has been removed

outcomes and implications of our waveform extraction methodology and draw some conclusions.

2 Materials and methods

2.1 Subjects

Data were collected from 12 healthy adult male volunteers, five at MCP Hahnemann University—Eastern Pennsylvania Psychiatric Institute (EPPI) Drexel University and seven others at the Biophotonics Laboratory, Bogazici University, Istanbul (with ages between 23 and 51 years). Participants were fitted for fNIRS monitoring after having given informed consent.

2.2 Measurements

Functional near-infrared spectroscopy measurements were taken with a custom-built system developed at Dr. Britton Chance's laboratory (University of Pennsylvania) and with its modified version, NIROXCOPE 201, developed at the Biophotonics Laboratory, Boğaziçi University. Details of this system and its probe configuration have been described in detail in our previous studies [2, 4]. Calculations of Hb and HbO_2 concentration changes have been performed by the well established ''modified Beer-Lambert law'' [12, 27, 31, 35]. There has been some controversy in the literature on whether neuronal activation should be monitored with Hb, HbO_2, Oxygenation (HbO_2–Hb), or total Hb (THb = HbO_2 + Hb) [1, 7, 10, 11, 15, 24, 27, 28, 32–34, 36]. While most of these studies stress that HbO_2 reflects neuronal activation more reliably and consistently, some others have shown that this effect is only global. In a study on simultaneous fNIRS–fMRI recordings [32], it was observed that the HbO_2 component exhibits the strongest correlation with the fMRI–BOLD signal; hence we have decided to concentrate on the HbO_2 data.

2.3 Experimental protocol

The procedure is a direct adaptation from McCarthy et al. [25] and is the similar one used in our previous studies [2–4]. It is a simple discrimination task, or ''oddball'' paradigm, in which subjects are presented with two stimuli in a Bernoulli sequence in the center of the screen. The participants are asked to press the left button of a mouse for non-targets (oddball) and right button for the targets, where target stimuli consist of ''XXXXX'' token on the screen versus the oddball case represented by the token ''OOOOO''. Overall, 1,024 stimuli are presented at 1.5-s intervals (total time, 25 min). The targets ''X'' are presented on 64 of the trials, that is, on the average, once every 16 trials, while the context oddballs ''O'' in the remaining 960 instances.

2.4 Pre-processing of the data

Duration of stimuli of both context and target types on the screen is 500 ms; hence there are blank intervals of 1 s. Recording is done at a sampling rate of 1.7 Hz, so that the Nyquist bandwidth is 0.85 Hz. We encountered some data acquisition defects such as clipping and saturation in the detector signals due to non-hermetic coupling and ambient light, and outliers due to head movements of subjects. We also observed that, in some cases, detectors gave poor measurement due to hair occlusions and/or due to sweating effect. Hence, due to detector defects described above, data from some of the detectors had to be excluded. There was no particular pattern of defective detectors [2].

Data were preprocessed with outlier elimination, low pas filtering, and detrending algorithms explained in our previous studies [2–4]. Finally, since our purpose is the extraction of waveforms associated with cognitive activity, we focus on the fNIRS segments that consist of the m samples taken just after the known target stimulus instants. In other words, we mask out the m sample intervals after the presentation of a target stimulus, and there are 64 such windowed segments per detector in an experiment.

2.5 ICA as a linear representation for fNIRS–HbO_2 signals

ICA is a linear transformation technique for the source separation of multidimensional data as described in [3, 14, 16]. As compared to other popular linear decompositions such as Gabor or wavelet analyses, ICA builds basis functions in a data-driven fashion and arrives at statistical independent projections or bases. Using higher order statistics (beyond second order), ICA estimates the basis in such a way that the projections of the observation data onto the basis vectors are mutually as independent as possible. The data-dependent nature of ICA makes it very useful especially for dimensionality reduction and transform coding, and this interpretation of ICA has proven very useful in image feature extraction for recognition applications [14, 16]. There are two complementary approaches to use and interpret ICA. In the first form, the emphasis is on the projection

weights, or equivalently independent components to encode the essential part of the multidimensional data. In the second form, actually used in the present work, the emphasis is on the basis vectors themselves in associating a neurophysiological interpretation with one or more of them. Accordingly, we conjecture that one of the ICA basis vectors estimated from evoked fNIRS–HbO_2 responses accounts for the generic waveform of the cognitive activity induced during a target categorization task. Similarly, the remainder of the basis vectors can be associated with other signal patterns corresponding to background activity of the brain, respiration and heartbeat artifacts, etc. From the perspective of a generative signal model, we find it fair to assume that the latter activities are independent from each other and from the cognitive activity. The short-time fNIRS–HbO_2 signals (the m-sample sequence from the stimulus instant until the vanishing of the response) are projected onto this basis set, such that the neurophysiological activations, i.e., projection weights, are statistically as independent as possible. Afterwards, we identify one of the basis vectors in this linear representation as the signal pattern conforming to brain cognitive activity model, called the Gamma pattern. We call this basis waveform as the fNIRS cognitive activity-related waveform, analogous to the brain hemodynamic response in the fMRI–BOLD setting. We have explored other signal-processing techniques, such as principal component analysis (PCA) that decorrelates projection weights based on their second-order statistics or spline smoothing followed by waveform clustering. However these alternative techniques, though yielding BOLD-like waveforms, were still inferior to ICA in capturing [3] the expected response waveform.

The basic ICA model is written as $\mathbf{x} = \mathbf{As}$, where $\mathbf{x}$ is the observation vector, $\mathbf{A}$ the basis matrix spanning a subset of the observation space. If $\mathbf{x}$ is m-dimensional and $\mathbf{A}$ consists of n linearly independent m-dimensional column vectors, the vector $\mathbf{s}$, which is the weight resulting from the projection of the observations $\mathbf{x}$ onto the columns of $\mathbf{A}$, is m-dimensional. In our scheme we want the components of the weight vector $\mathbf{s}$ to be independent. Each coefficient s_j quantifies the contribution of the jth basis vector (jth column of $\mathbf{A}$) in explaining the observation vector $\mathbf{x}$. The ICA algorithm induces any two such coefficients s_k and s_l, $k \neq l$ to be statistically ''as independent as possible''. Under these conditions, any observation sequence $\mathbf{x}$ is represented as a linear combination of the columns of $\mathbf{A}$. In the fNIRS–HbO_2 context, we associate the columns of the matrix $\mathbf{A}$ with candidate signal patterns related to neurophysiological activities. We conjecture that one or two bases, that is, columns of $\mathbf{A}$, correspond to cognitive activity of the brain. Other bases would be related to residual waveforms such as background activity, breathing and heartbeat artifacts, etc. In conclusion, our exploratory analysis focuses on resolving the fNIRS signal patterns into linear components. The details of the identification procedure are explained in Sect. 2.6.

Let $z(t)$ be an fNIRS–HbO_2 recording from a certain detector. In the aftermath of a stimulus, we pick m samples; for example, if a stimulus occurs at time t_k, the corresponding vector would read as $\mathbf{x} = [z(t_k), z(t_k + 1),...,z(t_k + m–1)]^T$. There are K target presentations, hence stimuli in the course of an experiment, occurring at instants t_k,$k = 1,...,K$ (see Fig. 2). A dataset matrix associated with a single detector $X^{\text{sensor}}_{\text{subject}}$ consists of concatenated m-component vectors of fNIRS–HbO_2 responses to each of the target stimuli arriving at respective t_k instants. The procedure is repeated for every detector of a given subject to obtain as many matrices $X^{\text{sensor}}_{\text{subject}}$ as the number of detectors, then data from four detectors of the same quadrant are concatenated further to form the dataset $X^{\text{quadrant}}_{\text{subject}}$ corresponding to a subject/quadrant pair.

Morren et al., used ICA based source separation in extracting the fast neuronal signal from a set of detectors placed 3 cm away from sources in a circumferential manner [11, 26]. Similar to their study, the ICA algorithm demands statistical independence of data and linearity. The independence of cerebral activity processes was stipulated; in fact there does not exist any plausible argument for the non-independence of cognitive reaction from brain's ongoing activity, and the independence of the former two from the artifacts. For linearity, on the other hand, we assume that different processes in the brain are homogeneously superposed in the fNIRS–HbO_2 signal. This assumption together with independence makes the use of ICA plausible in our problem. There exists one more application-dependent issue regarding the nature of observations $\mathbf{x}_k$. We assume that expectations of $\mathbf{x}_k$ can be replaced by its sample averages. The reason is that the specific ICA algorithm we have used (FastICA [16]) necessitates that negentropy be approximated with sample averages of the nonlinearly transformed random observations $\mathbf{x}$. In other words, the FastICA algorithm maximizes negentropy, which is an information-theoretic measure of non-Gaussianity, and this, in turn, maximizes independence between projection weights of ICA. Since, in the basic ICA model, the observed data $\mathbf{x}$ and the unobserved vector $\mathbf{s}$ are interpreted as stochastic processes, we should be able to replace expectations with sample averages so long as

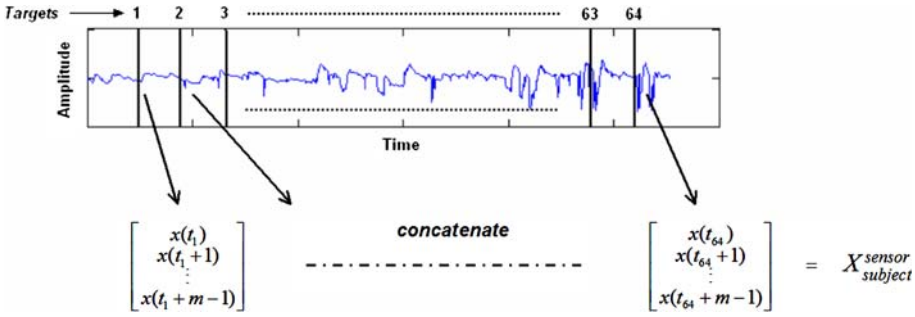

Fig. 2 An fNIRS–HbO_2 signal superposed with markers corresponding to targets instances t_k, $k = 1,...,K = 64$

the data **x** consists of or assumed to be independent identically distributed (i.i.d.) observations. Notice that the i.i.d. assumption, although not often questioned in practice, is common to any statistical method, e.g., in maximum-likelihood estimation [14].

2.6 Model-guided selection of cognitive response waveforms

The ICA algorithm outputs n basis vectors, but does not provide a natural ordering of them based on objective grounds such as energy content or saliency. There will always exist some ambiguity as to which waveforms, if any, correspond to the cognitive activity. Notice that one cannot use energy content or the variance of projection weights as a criterion. The PCA method would not be any more successful since the sought after cognitive activity forms a tiny fraction of the background. Analogous to fMRI–BOLD data analysis, this ambiguity can be resolved by considering the conformance of the waveforms to a predefined BHR model. This has been the common practice in fMRI studies [8, 13, 20, 21, 37] and recent NIR studies [18, 29–31].

The response model is the Gamma function (see Fig. 1) defined as

$$h(t) = \begin{cases} B(t-T)^2 \mathrm{e}^{-(t-T)/\tau} & \text{for } t \geq T \\ 0 & \text{for } t < T \end{cases} \qquad (1)$$

where τ is the time-constant that characterizes the reaction duration, B is the strength parameter, T is the delay in responding to the target stimulus, and t is now a continuous-time index. Let **h** be the vector with ith component $h(iT_s), i = 0,...,m-1$, the periodic samples of the model waveform in (1), where T_s is the sampling period. Any one of the identified components (say, the lth ICA basis vector) $\mathbf{a}_l = [a_l(0),a_l(1),...,(m-1)]^T$, $(l = 1,...,n)$, is qualified according to its matching degree to the waveform in (1), following the estimation of the parameters B, T and τ. Given the lth basis vector a_l, the B_l, T_l, τ_l parameters are estimated by a mean squared error procedure, i.e.,

$$\{B_l, T_l, \tau_l\} = \arg\min_{B,T,\tau} \sum_{i=1}^{m} [a_l(i) - h(i; B, T, \tau)]^2 \qquad (2)$$

In the following, we will assume that the parameters have been estimated, hence $\boldsymbol{h}_l = \mathbf{h}(B_l,T_l,\tau_l)$. Notice also that amplitude parameter B is allowed to take negative values in order to compensate for the sign ambiguity inherent to ICA. We set an upper limit to the reaction delay T, that is 3 s, and similarly the time constant τ is constrained to be in the range of (1, 4) [8, 22]. This signifies that the elapsed time between the 10% rise and decay instances of the BOLD signal have durations between extremes 6.5 and 25.9 s. The constrained minimization of (2) can be solved by such routines as in the Optimization Toolbox in MATLAB 7.0 (The MathWorks, Inc., MA, USA). Each of the estimated vectors $\mathbf{a}_l$, $l = 1,...,n$ here is the total number of basis vectors in the ICA representation is qualified as representative of the cognitive activity based on its correlation with the model $\mathbf{h}_l$ whose parameters are estimated based on (2). The waveform with index l possessing the highest normalized correlation coefficient, provided this correlation is above a threshold, is declared as the cognitive activity-related waveform.

3 Experimental results

We create different datasets with the intention to address the following issues: (1) do the estimated waveforms correspond indeed to a cognitive activity-related response or just to the brain's background activity? (2) Are there any inter-subject and/or inter-detector cohesion in the estimated waveforms? (3) How well does the ICA approach conform to the Gamma model?

We process detector quadrants of subjects separately as each group explores a different region of the

prefrontal cortex. Since there are four quadrants, four datasets per subject are possible, and this results in a total of 48 datasets for 12 subjects. The formation of any one dataset is as follows: each detector yields the responses from the $K = 64$ target stimuli; hence we collect $N = 4 \times K = 256$ response vectors from the four detectors, provided none is defective. The response to a target stimulus is the fNIRS–HbO_2 time segment of m samples following a stimulus, as depicted graphically in Fig. 2.

The extent of the signal segment subsequent to a stimulus (dimension of the fNIRS–HbO_2 vectors $\mathbf{x}_k$), is chosen as $m = 40$ samples, corresponding to an interval of 23.5 s. This interval is a natural choice since it corresponds to the mean inter-target interval (ITI), of 40 samples exactly. We want to reiterate at this point that the interval of 23.5 s between two observation vectors is long enough to preclude a cognitive response to interfere with its successor. In fact, the Gamma function model decays after 3–4 time constants, that is 10–15 s, and has negligible residue in the tail region.

3.1 Waveform extraction results via ICA

Each target is expected, in principle, to trigger some HbO_2 signal corresponding to cognitive activity, as depicted in Fig. 1. However, these waveforms cannot readily be observed in the measured signal due to many interfering components such as baseline drifts, breathing effects, arterial pulsations (see Fig. 3), called confounding factors and hence one must resort to more sophisticated methods to extract them.

As a preprocessing step to ICA decomposition, we reduce the dimensionality of the data vectors via PCA. Thus, after the principal component analysis, we keep the most energetic (highest variance) projections of the multivariate data, that is, according to the proportion of variance (PoV) criterion. When PoV was set to 90% for the fNIRS–HbO_2 vectors, the number of projections was found to be four, for all subjects. The projection of the raw data onto this subspace smoothes it and removes high frequency fluctuations. In addition, the subspace dimension fixes the maximum number of independent components (basis vectors). In retrospect, four basis vectors seem plausible since one expects one or two cognitive activity-related basis vector(s) and the remaining two or three to represent the baseline activity and artifacts. We have used the FastICA algorithm [16]. The parameters adopted are shown in Table 1.

To illustrate the case in point, let's consider a single dataset, which consists of 256 vectors from mid-left detectors of a subject (4 detectors × 64 target presentations = 256 fNIRS segments of 40 samples each). The FastICA algorithm is applied to these vectors to yield four basis vectors, such that the contributing coefficients or the projections of the data onto the basis exhibit ''statistical independence'' to the best possible extent. The four estimated basis vectors are shown in Fig. 4, where solid curves correspond to the ones best fitting to Gamma functions, and the thick bars mark the estimated delay T. Top left box in Fig. 4 corresponds to the basis vector that best fits the model function (with a correlation value of 0.90). Other basis vectors, in decreasing correlation order, are displayed in the remainder boxes of Fig. 4. Obviously the waveforms with low conformance to the Gamma function model do not appeal to our expectation of cognitive activity response, and hence they must somehow originate from the baseline activity or artifacts.

Table 2 gives the conformance figures (normalized correlation coefficient) of the best-fitting vectors to the Gamma model. For all datasets, the correlation coefficient has been found to be of the order of 0.9, suggesting that the ICA outputs are in agreement with the model cognitive waveforms (Gamma waveform). Two comments can be made for the estimated time-constants τ, which is the scale parameter of the Gamma model in Table 2.

1. *Scale parameter variation across quadrants* The scale parameter τ for the same subject takes comparable values in neighboring quadrants ($P > 0.05$).

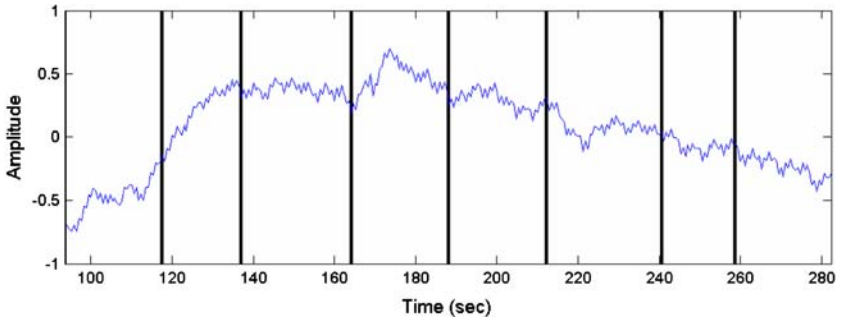

Fig. 3 A portion of fNIRS–HbO_2 signal during a session where eight targets are presented. *Thick bars* mark the arrival times of target stimuli. HbO_2 amplitude is in arbitrary units

Table 1 Parameters in ICA experiments

Parameter type	Parameter value
Time span of input vectors m	40
Number of measurements N	Per detector ≤ 64, per quadrant ≤ 256, per subject ≤ 1024
Number of ICA basis vectors n	4
Range of onset delay T	$T < 3$ s
Range of scale parameter τ	$1 < \tau < 4$

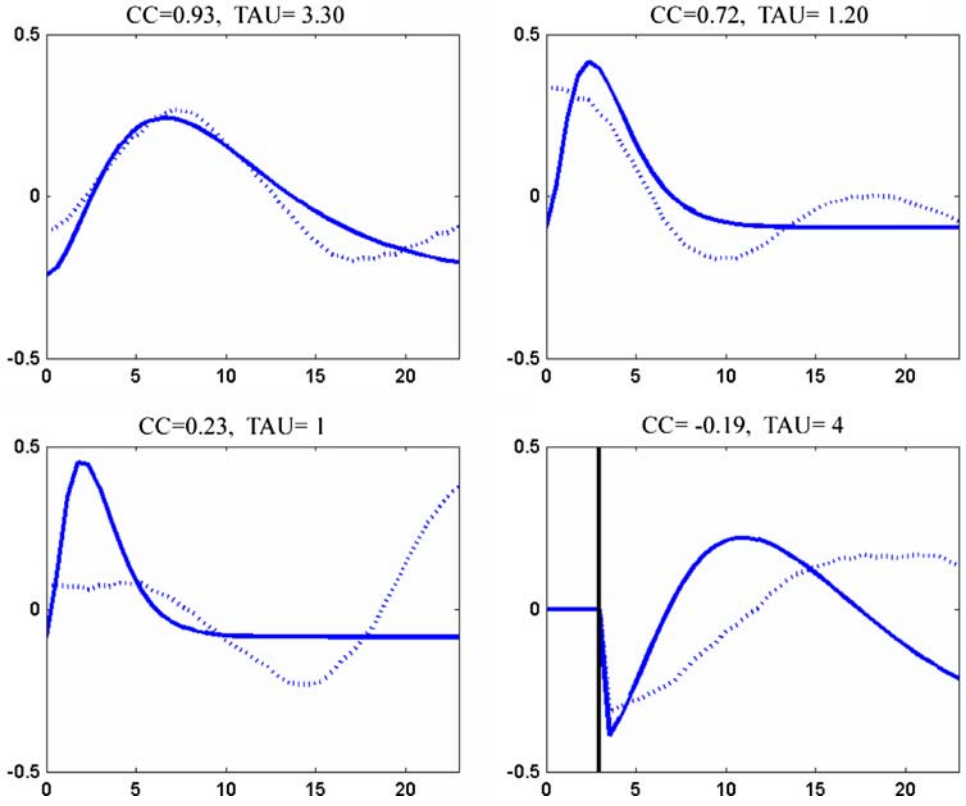

Fig. 4 The four ICA basis vectors of a given subject ranked in conformance degree (*CC* correlation coefficient, *TAU* estimated scale parameter). *Solid curves* depict the fitted Gamma function while the *dashed curves* depict the basis functions

Table 2 Correlation coefficients (*CC*) between best-fitting ICA basis vectors

Subject	Left (1–4)		Mid-left (5–8)		Mid-right (9–12)		Right (13–16)		Mean ± SD	
	CC	τ	CC	τ	CC	τ	CC	τ	CC	τ
1	0.94	2.17	0.94	3.61	0.89	2.74	0.84	2.22	0.90 ± 0.04	2.68 ± 0.58
2	0.98	2.81	0.92	1.28	0.96	1.55	0.92	1.28	0.94 ± 0.03	1.73 ± 0.63
3	0.84	4.00	0.83	3.92	0.82	4.00	0.88	1.53	0.84 ± 0.02	3.36 ± 1.06
4	0.89	1.81	0.92	4.00	0.85	1.00	–	–	0.89 ± 0.03	2.27 ± 1.27
5	0.97	3.29	0.97	3.66	0.92	1.82	0.88	3.23	0.94 ± 0.04	3.00 ± 0.70
6	–	–	0.93	3.17	0.92	3.37	0.92	2.97	0.92 ± 0.01	3.17 ± 0.16
7	0.74	1.56	0.82	2.77	0.81	3.25	0.75	1.11	0.78 ± 0.04	2.17 ± 0.87
8	0.95	4.00	0.89	1.72	0.96	2.60	0.95	4.00	0.94 ± 0.03	3.08 ± 0.97
9	0.93	3.30	0.90	1.91	0.90	2.44	0.90	1.41	0.91 ± 0.01	2.26 ± 0.70
10	0.82	2.38	0.88	2.05	0.86	2.24	–	–	0.85 ± 0.02	2.22 ± 0.13
11	0.89	1.90	0.95	1.88	0.88	1.02	0.85	1.23	0.89 ± 0.04	1.51 ± 0.39
12	0.92	2.67	0.85	1.47	0.73	3.44	0.85	4.00	0.84 ± 0.07	2.90 ± 0.95
Mean ± SD	0.90 ± 0.07	2.72 ± 0.81	0.90 ± 0.05	2.62 ± 0.97	0.88 ± 0.06	2.46 ± 0.93	0.87 ± 0.05	2.30 ± 1.10		

The scale parameter of the Gamma model (τ) (s) estimated with least-squares

However, there is no particular pattern of quadrants on which this observation consistently holds.

2. *Scale parameter variation across subjects* There is no agreement between scale parameters of different subjects, which was not expected in the first place. The subject-wise τ parameter was estimated from waveforms pooled from all detectors or from a subset of them, for example, all mid-left detectors. The variability of the τ parameter across quadrants for all subjects is statistically insignificant ($P < 0.1$).

Visual assessment of the basis vectors (estimated cognitive activity-related waveforms) is in line with the comments on τ values above. Figure 5 displays four responses per subject, one for each quadrant, and Fig. 6 displays responses of all the subjects per quadrant. Figure 5 suggests that, for the same subject, one obtains plausibly similar cognitive waveforms in different quadrants. Conversely, Fig. 6 shows that there can be significant waveform variations among subjects. One note of importance is the initial dip observed in most of the mid-right quadrant waveforms. Recall that the mid-right quadrant is adjusted such that it registers with the mid central gyrus of the prefrontal cortex, in particular the dorsa lateral prefrontal cortex, which is known to be the one of the most activated areas in an oddball task [25]. We also observe a post cursor undershoot of the HbO_2 activity, which has been shown to exist in other fMRI and fNIRS studies.

3.2 Waveform hunting in the rest-state data

It is an intriguing question; whether the extracted cognitive activity-related waveforms are produced as an artifact of the algorithm or not. To this effect, we carried out the same analysis on the rest-state data not involving any cognitive tasks. The subjects were in a supine position in a dimly lit quiet room, and were specifically asked to relax for a preparatory time interval. This rest data was similarly filtered in the 0.003–0.33 Hz range and detrended. As in Sect. 3.1, the ICA algorithm and Gamma waveform fitting were applied to 40-sample data vectors randomly positioned, similar to the oddball data. We have then estimated the distribution of CC's for the rest-state data. The CC scores are not expected to be very high, although even in the rest state, the brain is known to be not totally free of cognitive activity and HBO2 data might sporadically show Gamma waveform characteristics. Furthermore, detrending and filtering operations confine the HBO_2 time series within a spectral range from which it is not unusual for the ICA algorithm to extract Gamma-like bases.

A typical ICA basis vector from rest data and its corresponding best Gamma fit are shown in Fig. 7. We have compared the CC scores between the stimulated (oddball) and rest states by plotting their histograms in Fig. 8.

We can observe in Fig. 8, that the stimulated state fNIRS CCs are higher than those in the rest state data. The oddball CCs are centered on 0.88 with a standard deviation of 0.08 while the rest state CCs are centered on 0.62 with a standard deviation of 0.23. We have also checked the paired t test results. When we rank-ordered the CC scores for oddball and rest states we have found that their distributions are different with the probability of one. One use of the plot in Fig. 8 is in setting the threshold of demarcation between the two brain states. For example, when CC values are threshold at 0.825, the probability of false positives is 10%, that is, a spurious Gamma-like waveform occurs, leading us to believe in the existence of a cognitive response. The false positive occurrence is reduced down to 5% by shifting the threshold to CC = 0.85. The false negatives are respectively, 27.5 and 38%, that is the probability of missing an oddball stimulus event. We can argue that this imbalance between false positives and false negatives is acceptable since deciding for a cognitive activity is more misleading then missing some of them.

3.3 ICA waveform extraction versus grand averaging

In this part, we compare the performance of waveform extraction with straight coherent averaging vis-à-vis the ICA waveform extraction approach. We use the same dataset $X = \{\mathbf{x}_k\}$ formalism, where each m-vector $\mathbf{x}_k$ corresponds to a HBO_2 response waveform. Recall also that, in our experiments, we have considered such responses from a quadrant (four detectors) of a given subject to form a dataset X under the premise that these waveforms collectively characterize the cognitive activity in the monitored brain region. However, these single trial responses may not very well exhibit cognitive activity individually due to disturbing effects of background interference unrelated to the cognitive stimuli used. The conventional way to put into evidence the cognitive activity, if any, is to average all the normalized responses, i.e., after rendering the vectors zero mean and unit variance. We call this, the ''coherent average'' of waveforms, while the ICA output will be called as the ICA average, since the reconstruction of this waveform in the independent component subspace

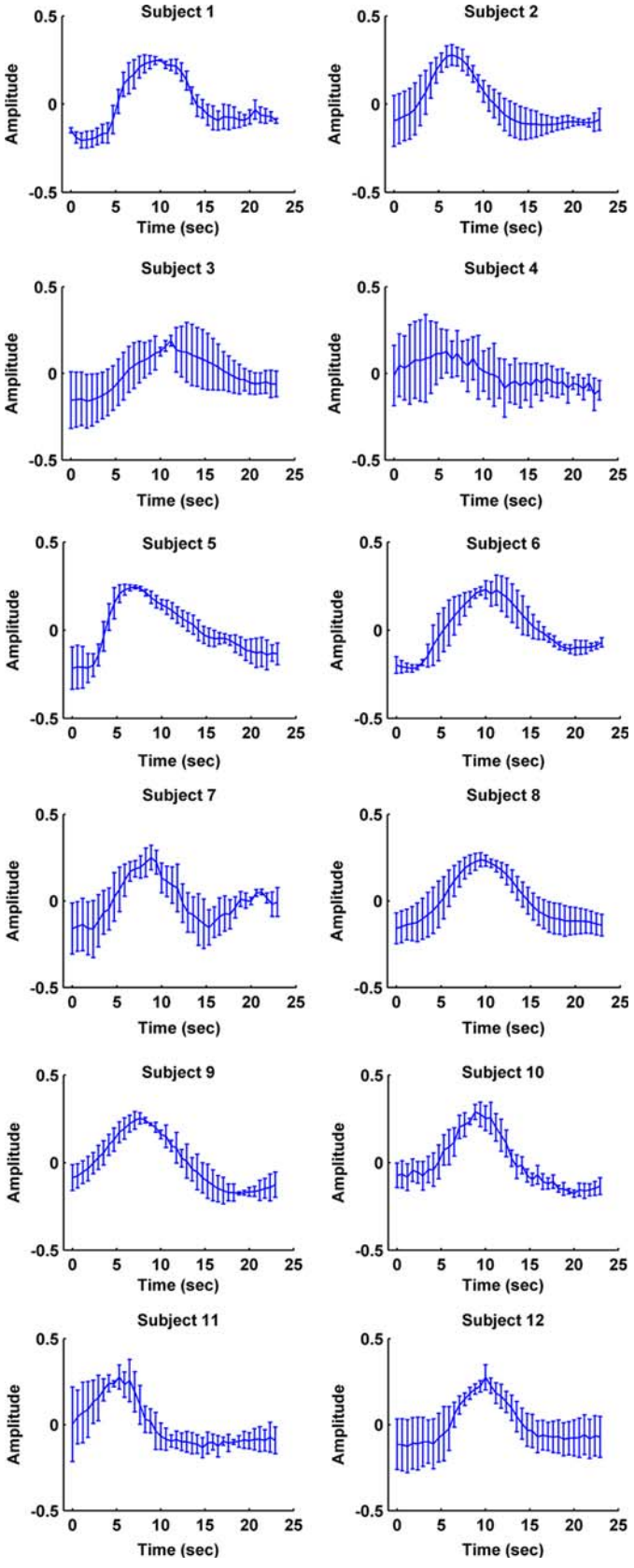

Fig. 5 *Error bar* plot for best-fitting ICA basis vectors averaged over quadrants per each subject (subjects 1–12). The *curve* shows the average over all quadrants, while the *bars* indicate the spread among the individual quadrant results

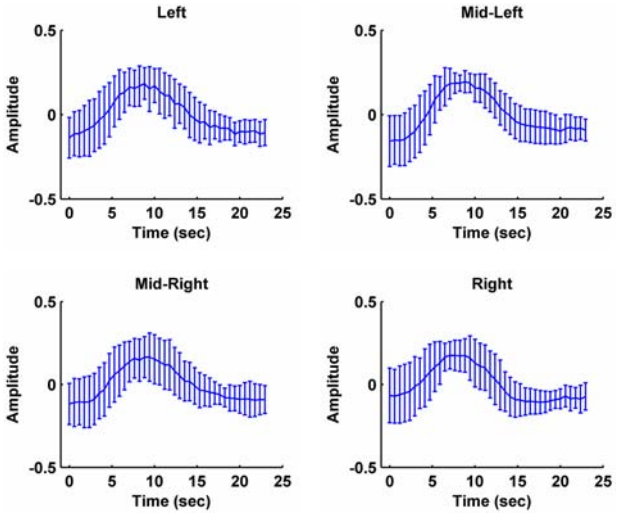

Fig. 6 *Error bar* plot for best-fitting ICA basis vectors averaged over subjects per each quadrant. The *curve* shows the average over all subjects, while the *bars* indicate the spread among them

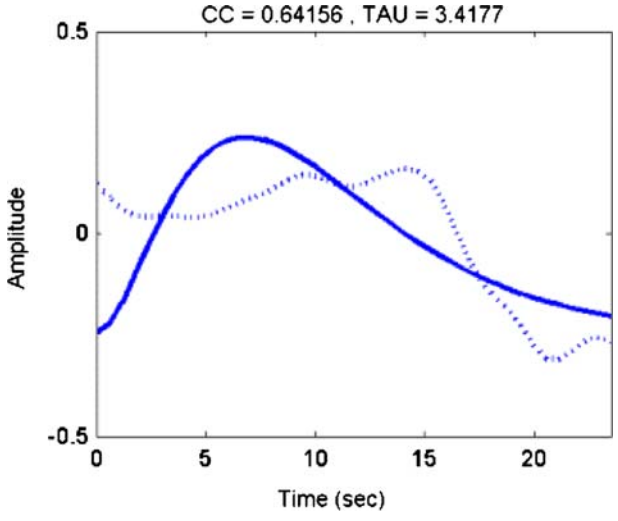

Fig. 7 One of the best ICA results from rest data

is intrinsically another type of averaging. We contrast the two approaches by superposing in Fig. 9a the averaged responses of Subject 2 mid-left quadrant, with the waveform extracted from the same dataset by ICA. This is a case where the two waveforms are compatible. However, this may not happen with all subject/quadrant pairs. A case in point is illustrated in Fig. 9b, where the coherent averaging does not result in a waveform plausibly related to cognitive activity. We conjecture that the HBO_2 signals were heavily embedded in background interference, much like the low contrast-to-noise ratio conditions in fMRI.

In this case, however, the ICA average achieves an 84% compatibility (in terms of correlation coefficient)

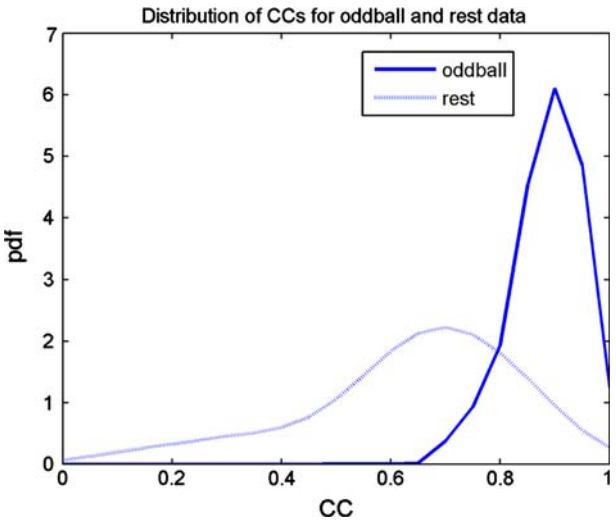

Fig. 8 Distribution of CCs for oddball and rest data

with a Gamma function (τ = 2.22 in Table 2). Thus the ICA waveform extraction can outperform the simple coherent averaging scheme, especially in the feeble signal and strong interference scenarios. Furthermore, ICA-guided averaging can be performed for selected waveforms that are positively correlated with the Gamma model. In other words, we select the waveforms that show positive correlation with the Gamma model output by the ICA approach, and then do coherent averaging on these raw waveforms. This more selective approach yields indeed an average waveform conforming to Gamma model than the plain coherent average. We display the advantage of ICA-guided averaging in Fig. 10a, b where the coherently averaged responses of Fig. 9a, b are compared against the ICA-guided waveform averaging results. In Fig. 10a, where the coherent average result is already satisfactory, coherent averaging of ICA-guided waveform instances has further smoothing effect on it. However, the effect of ICA-guided averaging is much more impressive in Fig. 10b. While direct coherent averaging does not yield a plausible waveform, the ICA-guided coherent averaging approaches the anticipated cognitive activity, mostly. We should note that the benefit of ICA guidance holds more or less for all subject/quadrant pairs.

Although the correlation of the extracted waveforms by ICA and the gamma function is expected to be strictly positive for all responses, it is a widely accepted fact that for impulse-like stimulus (like the one we have used in our experiments), the detectability of activations is hampered [22] by the dominance of the background interference or noise. A sudden increase in the heart rate or blood pressure might hinder the BHR,

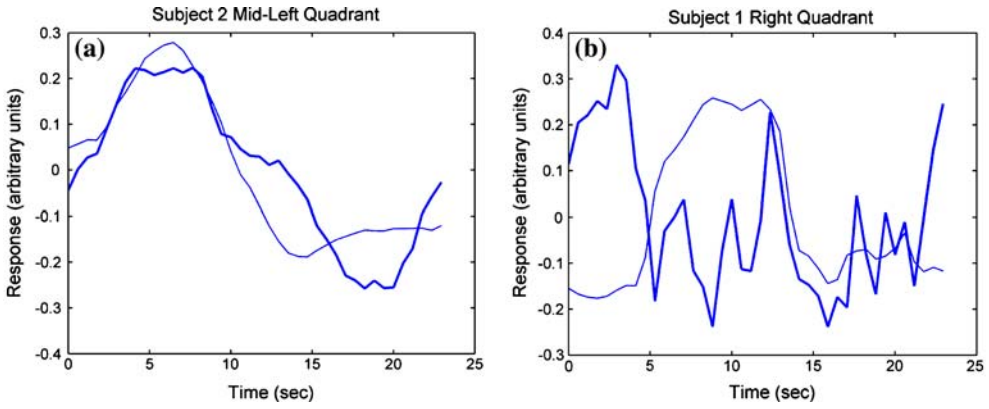

Fig. 9 **a** Coherent average (*thick*) and ICA average (*thin*) for Subject 2 mid-left quadrant. **b** Coherent average (*thick*) and ICA average (*thin*) for Subject 1 right quadrant

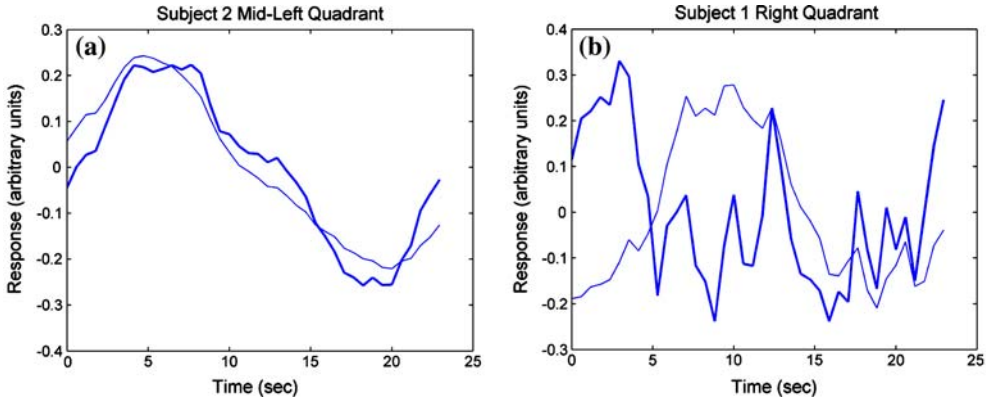

Fig. 10 **a** Coherent average (*thick*) and ICA-guided coherent average (*thin*) for Subject 2 mid-left quadrant. **b** Coherent average (*thick*) and ICA-guided coherent average (*thin*) for Subject 1 right quadrant

thereby lowering the chance of detecting it. For such responses, we think that a negative *spurious* correlation with the ICA waveform arises.

4 Discussion

The ICA method decomposes the data into its purportedly statistically independent components, which are composed of the superposition of baseline, cognitive response and other hemodynamic signals. The resulting ICA bases are qualified on a litmus test of similarity to the Gamma waveform, as being associated or not with cognitive activity. The remaining bases are then said to model background activity and artifacts of the brain. Since there is no evidence that contradicts neither linearity nor the independence assumption, we accept ICA as a plausible model.

An observation concerning the ICA methodology is that cognitive activity-related waveforms compatible with the Gamma model could be extracted from all detectors from all quadrants, albeit with varying success. A similar finding was observed by Morren et al., where an ICA component related to stimulus frequency was found in most of the channels with varying intensities [17].

For the sake of completeness, in our fNIRS–HbO_2 analysis, we find it useful to address the issue of i.i.d. assumption of the observations (or measurements). Specifically, in order to estimate the basis matrix $\mathbf{A}$ and the projection weights $\mathbf{s}$ using FastICA, any two observations $\mathbf{x}_k$ and $\mathbf{x}_l$, for $k \neq l$, should be independent identically distributed. This tacit assumption of i.i.d. measurement dataset $X = \{\mathbf{x}_k\}$ can be compromised by two factors: (1) spatial overlap of the support regions of $\mathbf{x}_k$ and $\mathbf{x}_l$ from adjacent detectors; (2) temporal overlap of responses of two successive stimuli, $\mathbf{x}_k$ and $\mathbf{x}_l$, obtained from the same detector. We shall discuss these aspects in the sequel:

4.1 Spatial i.i.d. conditions

First, in our experimental setup, the detectors within any one quadrant (see Fig. 3) are distant by at least 2.5 cm from each other, and in view of model diffusion geometry, these measurements can be considered as non-overlapping, hence potentially independent. Secondly, the ''identically distributed'' condition implies spatial homogeneity in the prefrontal cortex. This may not strictly hold, since not all prefrontal cortex regions give cognitive responses, but they all reflect invariably some background activity. For a

given subject and in the course of one type experiment (the same task), certain detectors will exhibit the cognitive response more favorably, certain others more or all of the background. Furthermore, in a study by Kirino et al. [19] the BOLD signals were extracted by averaging over 6×6 voxels, resulting in a cube of $18 \times 18 \times 42$ mm, which is commensurate with the resolution cell of fNIRS. Hence, the necessity in fMRI to average over a voxels neighborhood for statistically significant BOLD extraction [18, 26, 29–32] is tantamount to measure as diffuse an activity pattern as that in fNIRS detectors.

4.2 Temporal i.i.d. conditions

Time succession measurements from the same detector are non-overlapping since the average time interval between any two stimuli is 23.5 s. This is a long enough interval to preclude cognitive responses to interfere with their successors or predecessors, hence measurements can be considered temporally independent. In fact, the Gamma function model decays after 3–4 time constants, that is 10–15 s, and has negligible residue in the tail region. Temporal independence of responses is assumed also in fMRI analysis for BHR extraction [9]. As for temporal homogeneity, there is no guarantee that all single-event responses are alike in biological processes. In fact, in almost all EEG and fMRI time averaging processes, coherently or non-coherently, the individual event responses are not identical, but they are all assumed to belong to the same category of responses. Similarly, in fNIRS, we view the ICA scheme as a sophisticated indirect method of ''coherent averaging'' in the subspace designated by the ICA analysis. In conclusion, as in all coherent averaging experiments, we also assume temporal stillness during the course of an experiment, provided fatigue or other disturbing psychological factors do not play a role.

Another observation was the considerable variability of waveforms both within a subject and among subjects. This intra- and inter-subject variability of waveforms has also been observed by related studies in the literature. For example, Duann et al. [10] recommend the ICA approach for fMRI studies specifically for the reason of such intra- and inter variability of the hemodynamic response. Aguirre et al. [1], have reasoned that this variability might be due to physiological differences. Duann et al. [10], have shown that ''BOLD responses to infrequent presentations of flickering checkerboard stimuli may have time courses that vary systematically or unsystematically across stimulus parameters, visual brain areas, experimental sessions, and subjects''. We have also observed similar changes during the course of the whole experiment. Such variability or even the absence of the expected cognitive response may be attributed to the differences in the cerebrovascular physiology, attention level, and habituation of the subject [10, 33, 34].

To summarize the discussion, ICA proves to be a viable scheme in extracting cognitive activity-related waveforms. These estimated cognitive waveforms are in fact, the fNIRS counterparts of the brain hemodynamic response in fMRI. Furthermore, the theoretical underpinnings of ICA, in terms of i.i.d. measurements are satisfied. These waveforms, when parameterized, may provide quantifiable clues to the underlying brain processes.

5 Conclusion

With the goal of identifying the cognitive activity-related waveform to a single stimulus obtained by fNIRS, we explored a non-parametric method, namely independent component analysis. Our interpretation of ICA was to use it as a linear representation in exploratory terms, so its outcomes were benchmarked against a model waveform, the so-called Gamma waveform with time-constant parameter τ.

The first conclusion is that, waveforms estimated by ICA are plausibly related to cognitive activity, based on their conformance to the Gamma function model. Furthermore, we have shown that ICA waveform extraction outperforms coherent averaging in repeated experiments.

Our second conclusion was that the BOLD waveforms exhibit intra- and inter-subject variability. However, the intra-subject variability is much more subdued, and whether this waveform reproducibility is valid over time lapse experiments remains to be seen. On the other hand, one should beware from generalizing BOLD responses among the subjects.

Our work on fNIRS signal analysis continues with data collected from a larger set of subjects and on new protocols that include oddball experiments, lie experiments, Stroop tests and mental arithmetic tests. One interesting point to address is the ICA modeling of the B-spline coefficients for cognitive activity-related waveform extraction. In another experiment, EEG and fNIRS signals are concurrently recorded for emotion classification. Finally SPM: Statistical Parameter Method constitutes an alternative technique to label individual waveform portions as BOLD versus other activity signals.

Acknowledgments This work has been sponsored in part by funds from the Defense Advanced Research Projects Agency (DARPA) Augmented Cognition Program and the Office of Naval Research (ONR), under agreement numbers N00014-02-1-0524 and N00014-01-1-0986, in part by Boğaziçi University Research Fund, BURF 02S102, DPT 03K120250, and in part by TUBITAK-CNR Grant No. 104E101. The authors would like to thank Drs. Scott Bunce, Banu Onaral, Kambiz Pourrezaei, Meltem Izzetoglu, Britton Chance and Shoko Nioka and Mr Kurtulus Izzetoglu and Hasan Ayaz of Drexel University for sharing their fNIRS data with us.

References

1. Aguirre GK, Zarahn E, D'Esposito M (1998) The variability of human, bold hemodynamic responses. Neuroimage 8:360–369
2. Akgül CB, Sankur B, Akın A (2005) Spectral analysis of event-related hemodynamic responses in functional near infrared spectroscopy. J Comp Neuroscience 18:1, 67–83
3. Akgül CB, Sankur B, Akın A (2006) Extraction of cognitive activity related signals from functional near-infrared signals, 14th European Signal Processing Conference (EUSIPCO'06), Florence, Italy, September 4–8
4. Akin A, Bilensoy D, Emir UE, Gulsoy M, Candansayar S, Bolay H (2006) Cerebrovascular dynamics in patients with migraine: near-infrared spectroscopy study. Neurosci Lett 400:86–91
5. Andersen AH, Gash DM, Avison MJ (1999) Principal component analysis of the dynamic response measured by fMRI: a generalized linear systems framework. Magn Reson Imaging 17:795–815
6. Bandettini PA, Jesmanowicz A, Wong EC, Hyde JS (1993) Processing strategies for time-course data sets in functional MRI of the human brain. Magn Reson Med 30:161–173
7. Boas DA, Gaudette T, Strangman G, Cheng X, Marota JJA, Mandeville JB (2001) The accuracy of near infrared spectroscopy and imaging during focal changes in cerebral hemodynamics. Neuroimage 13:76–90
8. Boynton GM, Engel SA, Glover GH, Heeger DJ (1996) Linear systems analysis of functional magnetic resonance imaging in human V1. J Neurosci 16:4207–4221
9. Ciuciu P, Poline J-B, Marrelec G, Idier J, Pallier C, Benali H (2003) Unsupervised robust non-parametric estimation of the hemodynamic response function for any fMRI experiment. IEEE Trans Med Imaging 22(10):1235–1251
10. Duann JR, Jung TP, Kuo WJ, Yeh TC, Makeig S, Hsieh JC, Sejnowski TJ (2002) Single-trial variability in event-related bold signals. Neuroimage 15:823–835
11. Elwell CE, Cope M, Edwards AD, Wyatt JS, Reynolds EOR, Delpy DT (1992) Measurement of cerebral blood flow in adult humans using near infrared spectroscopy—methodology and possible errors. Adv Exp Med Biol 317:235–245
12. Firbank M, Okada E, Delpy DT (1998) A theoretical study of the signal contribution of regions of the adult head to near infrared spectroscopy studies of visual evoked responses. Neuroimaging 8:69–78
13. Friston KJ, Jezzard P, Turner R (1995) The analysis of functional MRI time-series. Hum Brain Mapp 1:153–171
14. Hastie E, Tibshirani R, Friedman J (2001) The elements of statistical learning. Springer Series in Statistics
15. Hoshi Y, Kosakab S, Xiec Y, Kohria S, Tamura M (1998) Relationship between fluctuations in the cerebral hemoglobin oxygenation state and neuronal activity under resting conditions in man. Neurosci Lett 245:147–150
16. Hyvärinen A, Karhunen J, Oja E (2001) Independent component analysis. Wiley, New York
17. Izzetoglu K, Bunce S, Ayaz H, Devaraj A, Onaral B, Pourrezaei K (2005) Functional near-infrared neuroimaging. IEEE Trans Neural Syst Rehabil Eng 13:153–159
18. Kennan RP, Horovitz SG, Maki A, Yamashita Y, Koizumi H, Gore JC (2002) Simultaneous recording of event-related auditory oddball response using transcranial near infrared optical topography and surface EEG. Neuroimage 16:587–592
19. Kirino E, Belger A, Goldman-Rakic P, McCarthy G (2000) Prefrontal activation evoked by infrequent target and novel stimuli in a visual target detection task: an event-related functional magnetic resonance imaging study. J Neurosci 20(17):6612–6618
20. Kruggel F, Herrmann CS, Wiggins CJ, von Cramon DY (2001) Hemodynamic and electroencephalographic responses to illusory figures: recording of the evoked potentials during functional MRI. Neuroimage 14:1327–1336
21. Kruggel F, von Cramon DY (2001) Nonlinear regression analysis of the hemodynamic response in functional MRI. Pattern Recognit Lett 22:1247–1252
22. Liu TT, Frank LR, Wong EC, Buxton RB (2001) Detection power, estimation efficiency, and predictability in event-related fMRI. Neuroimage 13:759–773
23. Marrelec G, Benali H, Ciuciu P, Pélégrini-Issac M, Poline J-B (2003) Robust Bayesian estimation of the hemodynamic response function in event-related BOLD fMRI using basic physiological information. Hum Brain Mapp 19:1–17
24. Mayhew J, Johnston D, Berwick J, Jones M, Coffey P, Zheng Y (2000) Spectroscopic analysis of neural activity in brain: increased oxygen consumption following activation of barrel cortex. Neuroimage 12:664–675
25. Mccarthy G, Luby M, Gore J, Goldman-Rakic P (1997) Infrequent events transiently activate human prefrontal and parietal cortex as measured by functional MRI. J Neurophysiol 77(3):1630–1634
26. Morren G, Wolf U, Lemmerling P, Wolf M, Choi JH, Gratton E, Lathauwer LD, Huffel SV (2004) Detection of fast neuronal signals in the motor cortex from functional near infrared spectroscopy measurements using independent component analysis. Med Biol Eng Comput 42:92–99
27. Obrig H, Wenzel R, Kohl M, Horst S, Wobst P, Steinbrink J, Thomas F, Villringer A (2000) Near-infrared spectroscopy: does it function in functional activation studies of the adult brain. Int J Psychophysiol 35:125–142
28. Obrig H, Neufang M, Wenzel R, Kohl M, Steinbrink J, Einhaupl K, Villringer A (2000) Spontaneous low frequency oscillations of cerebral hemodynamics and metabolism in human adults. Neuroimage 12:623–639
29. Obrig H, Neufang M, Wenzel R, Kohl M, Steinbrink J, Einhaupl K, Villringer A (2000) Spontaneous low frequency oscillations of cerebral hemodynamics and metabolism in human adults. Neuroimage 12:623–639
30. Prince S, Kolehmainen V, Kaipio JP, Franceschini MA, Boas D, Arridge SR (2003) Time-series estimation of biological factors in optical diffusion tomography. Phys Med Biol 48:1491–1504
31. Schroeter ML, Bücheler MM, Müller K, Uludağ K, Obrig H, Lohmann G, Tittgemeyer M, Villringer A, von Cramon DY (2004) Towards a standard analysis for functional near-infrared imaging. Neuroimage 21:283–290
32. Strangman G, Culver JP, Thompson JH, Boas DA (2002) A quantitative comparison of simultaneous BOLD fMRI and NIRS recordings during functional brain activation. Neuroimage 17:719–731

33. Toronov V, Franceschini MA, Filiaci ME, Wolf M, Fantini S, Gratton E (2000) Near-infrared study of fluctuations in cerebral hemodynamics during rest and motor stimulation: spatial mapping and temporal analysis. Med Phys 27:801–815
34. Toronov V, Webb A, Choi JH, Wolf M, Safonova L, Wolf U, Gratton E (2001) Study of local cerebral hemodynamics by frequency-domain near-infrared spectroscopy and correlation with simultaneously acquired functional magnetic resonance imaging. Opt Express 9(8):417–421
35. Villringer A, Chance B (1997) Non-invasive optical spectroscopy and imaging of human brain function. Trends Neurosci 20:4435–4442
36. Watanabe A, Matsuo K, Kato N, Kato T (2003) Cerebrovascular response to cognitive tasks and hyperventilation measured by multi-channel near-infrared spectroscopy. J Neuropsychiatry Clin Neurosci 15(4):442–449
37. Worsley KJ, Friston KJ (1995) Analysis Of fMRI time-series revisited-again. Neuroimage 2:173–181